Metal Oxide nanostructures-based Gas Sensors

Neeraj Goel[a], Kishor Kunal[a], Aditya Kushwaha[a], Mahesh Kumar[b, *]

[a]*Department of Electronics and Communication Engineering, Netaji Subhas University of Technology, Dwarka, New Delhi 110078, India*
[b]*Department of Electrical Engineering, Indian Institute of Technology Jodhpur, Jodhpur 342011, India*

Abstract

The usage of the gas sensor has been increasing very rapidly in the industry and in daily life for various potential applications. In recent years, metal oxide semiconductors (MOS) become the primary choice for designing highly sensitive, stable, and low-cost real-life applications-based gas sensors due to their inherent physical and chemical properties. Researchers have proposed numerous sensing mechanism to explain the functionality of MOS based gas sensors. In this review, we have comprehensively covered different sensing mechanisms used for MOS. We have also discussed different parameters affecting the sensitivity and selectivity of the gas sensors. Moreover, the different techniques used to enhance the gas sensing response of MOS based sensors are also extensively covered. And finally, we give our prospective on recent opportunities and challenges on future applications of MOS based gas sensors.

Keywords: *Metal oxide semiconductors (MOS), gas sensors, sensing mechanism, heterojunction.*

Corresponding Author

[*]E-mail: mkumar@iitj.ac.in

1. Introduction

In today's world, we want to expand the limit of our perceptions. To broaden the limit, a large number of sensors are developed. Gas sensor is a device that can detect a specific gas even if the amount or concentration of gas is very small [1, 2]. Sensor can help us in identifying the information in our surrounding which is relevant to us and also convert this information into electric signals [2, 3]. Gas sensors have been widely used in monitoring industry and domestic environments [4]. These sensors have several advantages such as low power consumption, small size, low cost, and high reliability. The demand of gas sensors is increasing day by day, hence we need the gas sensors with high sensitivity and better selectivity [5, 6]. The sensing material is one of the deciding factors about the performance of gas sensors. The gas sensing industry is dominated by metal oxide semiconductors (MOS) to fulfil the requirement of ideal gas sensors. MOS based gas sensors have many applications such as environmental monitoring, fire detection, detection of harmful gases in mines, home safety, traffic safety, and healthcare, as shown in Figure 1 [3, 7, 8].

In recent years, MOS gas sensors are one of the most researched groups of sensors particularly with the nanoscale size of 1 -90 nm due to their size dependent properties. The ratio between surface area and their volume increases drastically with decrease in material size. Moreover, the size and materials geometry affected the movement of electrons and holes in the nanomaterials [5, 9]. Over the past few years, a wide variety of gas sensors (catalytic-type, Electrochemical-type, MOS type) emerges based on distinct sensing mechanism and sensing materials. Among all the gas sensing materials, MOS sensors performance is higher because of their unique structures, physical and chemical properties. MOS based gas sensors could detect the gases even in ppt range, whereas the other kinds of sensors could not perform only in ppb or ppm ranges, as shown in Figure 2. The most often used MOS sensing materials are ZnO, SnO_2, MoO_3, TiO_2, WO_3, NiO, and Cu_2O [10-16]. Furthermore, in high-temperature or harsh situations, these MOS have better stability and response times, which is prerequisite for practical applications [5]. The material's popularity on the market is further aided by low-cost and easy production procedures [17, 18].
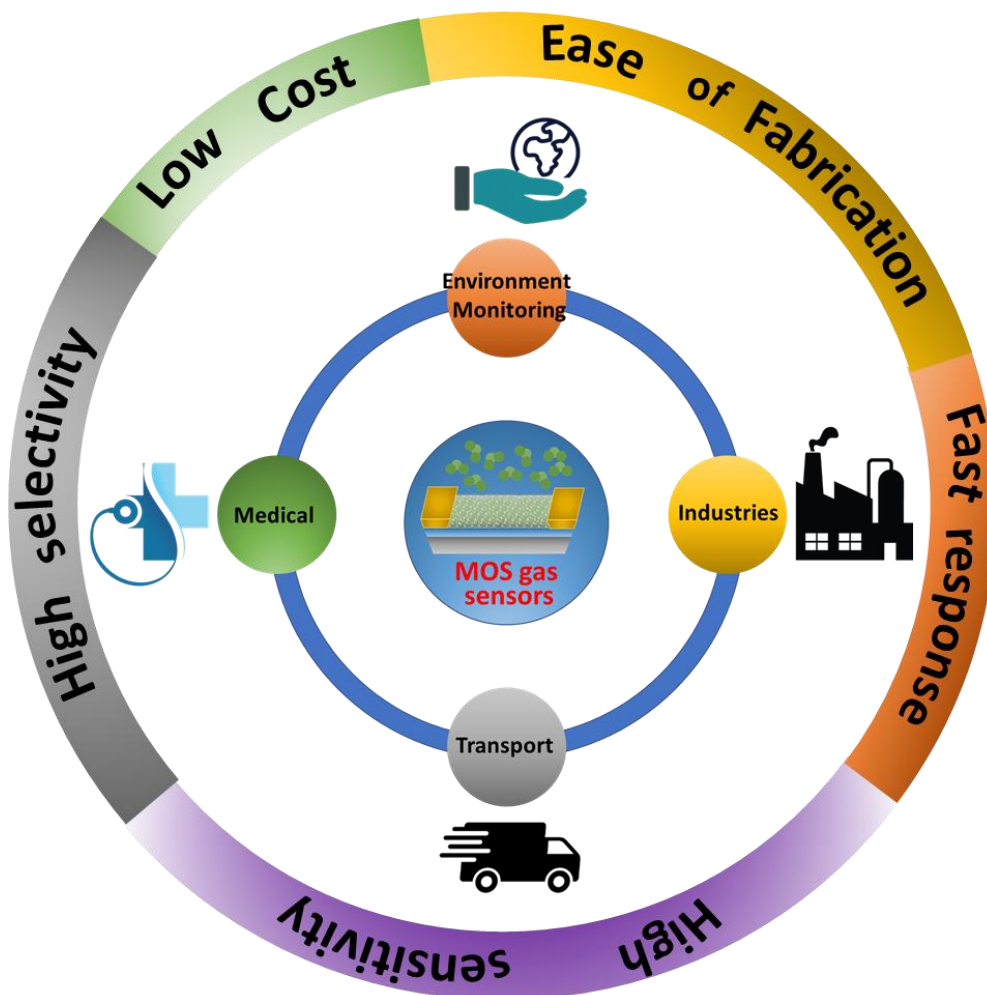
Figure 1. Application of MOS based gas sensors in various fields and their inherent characteristics for developing efficient gas sensors.
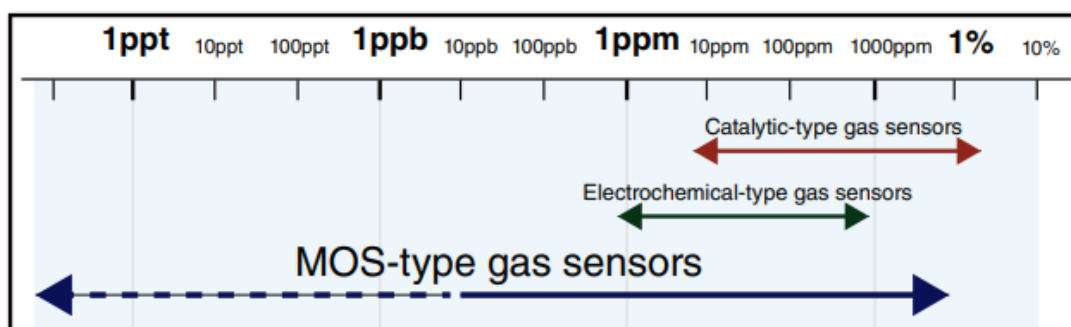

Figure 2. Sensing range comparison of catalytic-type, electrochemical-type and MOS-type gas sensors[19].

This review paper gives the brief idea about the MOS gas sensor. This is mainly focused on those

parameters which defines the gas sensors performance, sensing mechanism, methods to improve the gas sensing, and sensing related properties of the MOS. In this article, we have also discussed about the role of heterojunction and noble metal dopants in improving the gas sensing which is heavily used for developing high performance gas sensors.

2. Performance parameters of gas sensors

Performance of any gas sensor can be defined by several parameters such as sensitivity, stability, response and recovery time, selectivity, and operating temperature. Ideal gas sensor should have the high sensitivity and selectivity, good stability, long life cycle, low operating temperature, and fast response and recovery time [20-23].

Sensitivity: Gas sensor sensitivity is defined as the ability to sense gases. The slope of the response curve (also known as the calibration curve) is typically used to determine the sensitivity. The response curve is a plot between the device response and concentration of gas [24, 25]. A steeper slope indicates high sensitivity while a moderate slope signifies a lower sensitivity. In general, the normalized ratio of response signal over baseline is called the sensitivity of the gas sensors.

Selectivity: The selectivity of a gas sensor can be explained as the ability to sense target gas in presence of other gases. Ideal gas sensor has high selectivity indicating that it mainly senses the target gas and neglecting the other interfering gases. Hence, high selectivity confirms that the sensor gives the accurate information about the existence and concentration of gases.

Stability: Stability indicates the ability of a sensor to produce reliable results over a period of time. MOS based gas sensors has low stability that leads to the undesired result or false alarms. To some extent stability can be improved by lowering the operating temperature.

Response time: The time taken by the gas sensor to reach 90% of the saturation value after the triggering is called response time. Logarithmic curve and error function are the common approximations used for the transient response shape [22].

Recovery time: The time taken by the gas sensor to reach 90% of the initial value after 'off' the triggering is called the recovery time.

Operating temperature: Ideally, the room temperature-based gas sensors are preferred in most of the practical applications due to their less power consumption, high durability, and easy portability. However, in most of the MOS based gas sensors, high temperature is required to activate the absorption/desorption process at the sensing surface.

3. Gas sensing mechanism

Based on the operating temperature, MOS can be classified into two categories, the first category involves the materials which follow the surface conductance effects while the second category comprises the materials which follow the bulk conductance effects [5]. The first category belong to the oxides operated at low to moderate temperature (<600°C) whereas the second category works at very high temperature (>700°C) [5, 26]. The operating temperature also defines the mechanism by which these materials functions. Among popular MOS, SnO_2 and ZnO are some of the oxides which belongs to the first category and called as surface conductance materials. Bulk conductance effect is slow at the lower temperature and change in conductance occurs because of the adsorption and removal of oxygen at the surfaces [26]. Some examples of the bulk conductance materials (BCM) are TiO_2, Nb_2O_5. These BCM belongs to the second category and only respond to variation in the partial oxygen pressure at higher temperature (>700°C). They also showed equilibrium between the atmosphere and bulk stoichiometry [26].

MOS based gas sensors detect the presence of gases primarily by recording the changes occurring in the electric properties due to the target gas which is in contact with the sensor. The sensing mechanisms explain the physics affecting the electric properties of a gas sensor upon exposure of target gas molecules. The MOS based gas sensing mechanisms can be categorized at microscopic and macroscopic levels. The microscopic perspective explains various mechanism such as Fermi level control theory and charge carrier depletion layer theory. While the macroscopic mechanism focuses on the relationship between the gases and materials. The macroscopic level involves adsorption/desorption processes, bulk resistance control mechanism and gas diffusion control mechanisms. In most of the MOS based gas sensors, macroscopic level is used to explain the gas sensing mechanisms.
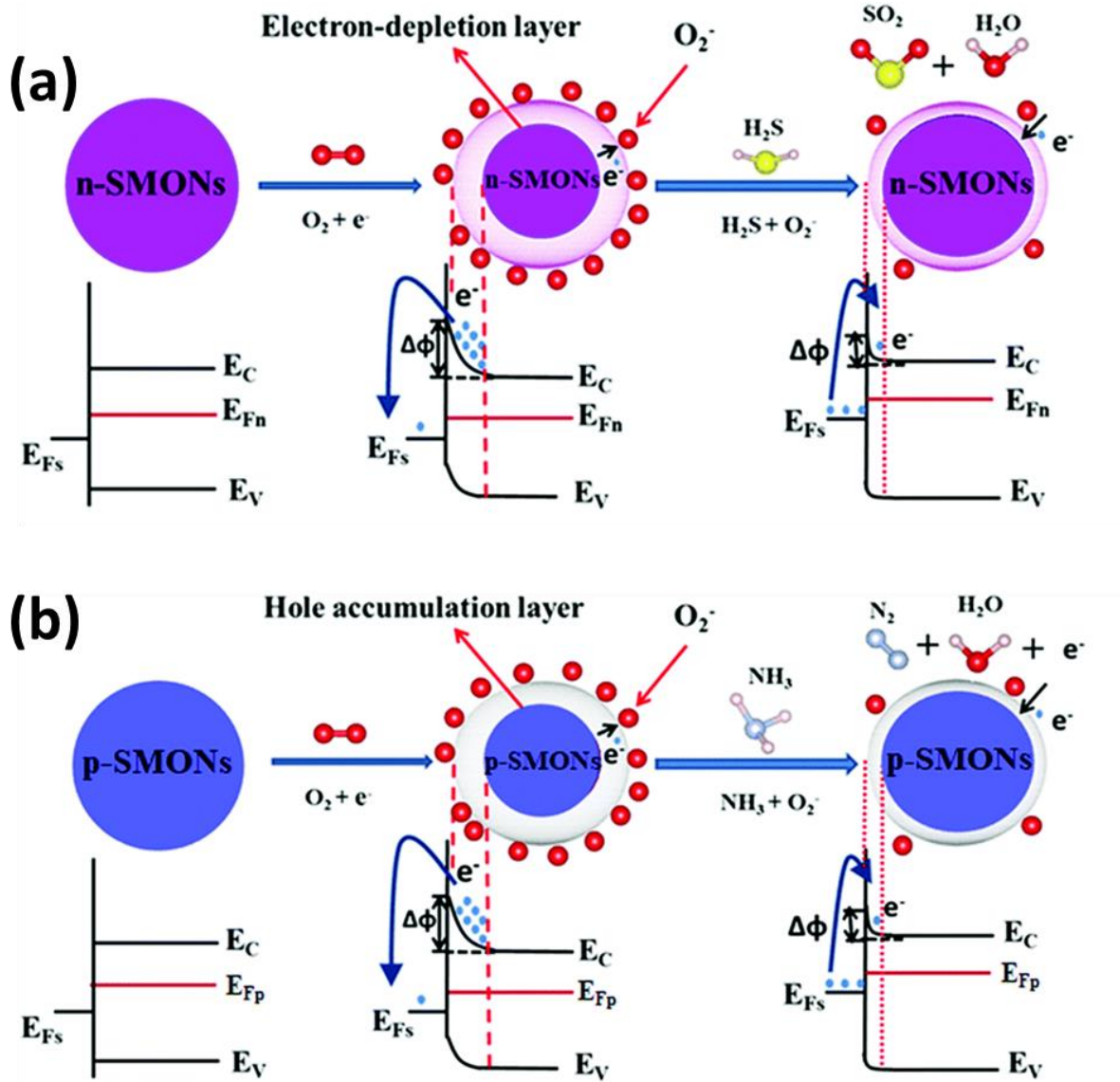
When different gases come in contact with the MOS, the conductivity and work function of the MOS changes significantly. Most of the gas sensing mechanisms work on the adsorption/desorption principle. The adsorption/desorption processes explain the physical or

chemical changes in the sensor behavior when the gas is in contact with the sensing surface. Upon exposure of target gas molecules, resistance of the material changes because of the concentration of charge carrier changes in a significant manner. The carrier concentration changes ascribed to chemisorption and physisorption process of target gas molecules and ambient oxygen molecules.

Chemical Adsorption/Desorption is one of the dominant gas sensing mechanisms and strongly affect most of the MOS based gas sensing devices. When gas comes into direct contact with the sensor, a chemical reaction happens, causing an electrical signal to change. This change might occur due to the presence of targeted gas or ambient oxygen molecules. The oxygen adsorption is one of the most common gas sensing mechanisms and strongly affect most of the MOS based gas sensing devices. When MOS is brought into air, the oxygen molecules started to adsorb on the material surface and an oxidizing or reducing reaction took place between the atmospheric oxygen and sensing surface. Based on these reactions, some electrical properties or resistance of the sensing material changes considerably. Various kinds of oxygen ions (O_2^-, O^-, O^{2-}) are formed in according with the operating temperature after capturing the electrons from the sensing materials. Hence, the conductivity/resistance of the sensing material changes due to change in surface electron density. Upon exposure of reducing targeted gases on n-type MOS, the captured electrons by oxygen species released back to sensing material leading to decrease in resistance, as shown in Figure 3(a). The reduction in the value of resistance could further be confirmed by decreased barrier height ($\Delta\phi$) at the interface. While in presence of oxidizing gases, the electron density decreases further resulting in increasing the value of resistance. In contrast, upon adsorbing of reducing gases on p-type MOS surface, reduces the hole accumulation layer due to electron-hole recombination process, as depicted in Figure 3(b). As a result, the surface resistance increases of the p-type MOS structure. However, in presence of oxidizing gases on p-type MOS, the hole carrier concentration significantly increases due to trapping of electrons by the oxidizing gases and hence the value of resistance decreases.

In addition to chemisorption process, physisorption also play a very important role in understanding of gas sensing mechanism. According to physical adsorption process, gas molecules is adsorbed at the surface of MOS material via coulomb forces and other different type of intermolecular forces without any chemical changes. Physical adsorption causes a minor

difference in the conductivity of MOS materials, hence this process is not commonly used to explain the gas sensing mechanism [27-29]. Humidity sensors are the most common MOS-based sensors, whose sensing mechanism is based on the physical adsorption/desorption processes [30]. Therefore, chemical adsorption is considered as the dominant gas sensing mechanism in the majority of MOS based gas sensors.

E_C: bottom of conduction band; E_V: top of valence band; E_{Fn}: bulk Fermi level; E_{Fs}: surface Fermi level; $\Delta\varphi$: potential barrier;

Figure 3. Gas sensing mechanism of (a) n- and (b) p-type semiconducting metal oxide nanostructures (SMONs) upon exposure of reducing gases.

Moreover, the resistance of MOS based gas sensors could also be changed due to the phase transformations of the gas sensing material. However, this mechanism is only applicable for limited gas sensing materials, such as ABO_3 type MOS composites [31]. α-Fe_2O_3 and γ-Fe_2O_3 are the two different type of phase composition of Fe_2O_3 samples which is prepared by the heating of $FeFe(CN_6)$ [32]. Based on the two different phases of the material and their combined phases, gas sensing experiments were conducted, and various gas sensing mechanisms of two samples of Fe_2O_3 were investigated. In the case of α-Fe_2O_3, the phase structure was relatively stable, therefore typical O_2 adsorption model can describe the gas sensing mechanism of α-Fe_2O_3. Moreover, due to the changes in the inside structure of γ-Fe_2O_3 its resistance changes [33]. Hence, α-Fe_2O_3 and γ-Fe_2O_3 possess different gas sensing properties despite their identical morphological structures. Gao et al.[34] have also demonstrated that WO_3 hydrogen gas sensing films stability strongly affected by the phase transition. The materials present originally as W_3O_{12} clusters form and by sharing the W-O-W bonds at corner. This whole transition affects the H_2 desorption energy and the HOMO-LUMO gap, resulting in bulk resistance change and improved sensing performance.

In the gas sensing process, materials and gases are the critical components. The chemisorption and physisorption processes are primarily reliant on the chemical and the physical characteristics of that material. In addition, there are some mechanisms largely relying on the process of gas diffusion. Several theories are proposed by scientists indicating that the gas diffusion controls the sensitivity of semiconductor based gas sensors [35-37]. For better understanding of gas sensing properties, Wang et al. have developed a canal and hollow sphere model [38]. When the temperature is less than 150 °C then adsorbed O_2 at the SnO_2 surface was poorly reactive O^{2-} ions, therefore surface chemical reaction controlled the gas sensing reaction. Now some amount of the target gas is oxidized partially, and the remaining part of target gas diffuses into inner pores and undergo some chemical reactions. When the temperature is in the range of 150 °C to 200 °C or greater than 200 °C, then O^- and O^{2-} are the formed, so surface chemical diffusion process is more active now. Hence, complete oxidation and ionization of target gases inside the hollow sphere improves the sensing response [39-41].

8

4. Methods to improve gas sensing

Gas sensors are mainly used to detect the harmful gases which are threat to human health even at a very low concentration. Therefore, highly sensitive and selective gas sensors are prime need of the electronic industry [42-45]. The adsorption of gas molecules on the sensing surface could significantly be improved by increasing the number of adsorption sites, increasing the oxygen vacancy, and by enhancing the surface catalytic activity. Moreover, in the case of electron depletion layer/ hole accumulation layer [46, 47], gas sensing could be improved by barrier reducing and also by the increasing the flow of electrons . Some of the methods to improve the gas sensing are:

4.1 Doping with noble metals

Introducing noble metals is one of the most effective and widely used methods for fast catalytic chemical reactions. Normally, Au, Ag, Pt and Pd are some of the noble metal dopants used for improving the gas sensing response in the case of MOS sensing materials. There are several steps involved to explain the role of noble metals in improving the sensing response. Firstly, adsorption activation energy is decreased, and adsorption of additional oxygen anions and analyte gas molecules occurs. Secondly, the redistribution of excitons causes the band bending and created a Schottky barrier at the interface, which alters the movement of charge carriers. Lastly, activation energy of the process is lowered by the spillover impact. Due to the addition of the noble metal dopant, the adsorption capacity of gases increases. For example, In the case of $W_{18}O_{49}$, when Pd was added then it adsorbed H_2 approximately 900 times of its own volume. Due to this greater adsorption, the effective collision frequency between gas molecules also increased significantly [48]. In other terms, due to this development, the adsorption energy would get decreased after adding the noble metal dopant.

Xue et al. demonstrated the sensing behavior of pristine SnO_2 and Pt-SnO_2 upon exposure of CH_4 molecules through first-principle calculations[49]. The adsorption energy of oxygen on the SnO_2 and Pt-SnO_2 are -0.92 eV and -1.32 eV, respectively, on the exposed crystal planes (110). The obtained results showed that the adsorption of oxygen molecules was more on the noble metal modified SnO_2 as compared to pristine SnO_2. From Figures 4 (a) and (b), it can be clearly visible that adsorption energy is decreased remarkably for all the three adsorption sites when SnO_2 is

doped with Pt, confirming that CH_4 is more adsorbed on the surface of Pt-SnO_2 as compared to the SnO_2 [50-52].

Moreover, in most of the cases, the work function of MOS gas sensitive materials is less than the noble materials, therefore redistribution of charge is necessary for achieving the equilibrium. Once the physical contact between metal and MOS is made, the band bending due to charge transfer at the interface formed a Schottky barrier at the junction of MOS and noble metals. The conduction band electrons of MOS sensing material moved into the noble metal particles and form a layer called dipole layer interface (Figure 4(c)). This layer at the interface prevents the electron-hole pair recombination process, therefore the MOS's gas response is increased. This phenomenon is called electronic sensitization [53-56].

Figures 4(d-f) provide an illustration of the factor contributing to the excellent sensing qualities, which has to do with the incorporation of Au-doped atoms. To enhance the chemo-resistive gas sensors' sensing capabilities, metal catalysts such as Au, Pd, Pt, and Ag were frequently utilized. The sensing film functionality was enhanced by catalytic processes on the nanosensors material, which also lead to excellent gas sensor characteristics (such as sensitivity, selectivity, and response and recovery times) [57-60]. The two different methods (i.e., electro-chemical sensitizations) explain why Au nanoparticles have improved sensing performance [61, 62]. The mismatch in the work functions of Au (i.e., $\Phi_{Au} = 5.1eV$) and WO_3 (i.e., $\Phi_{WO3} = 5.7$ eV), which causes the electrical sensitization, leads to a rise in base resistances as seen in Figure 4(g) [63]. According to Figure 4(f), the electron transmission from semiconducting WO_3 to the Au nanoparticles results in an enhancement in resistance, which is implied by an increment in the sizes of the electron depletion zones. Consequently, there were fluctuations in resistance of WO_3 nanosheet due to the treatment of NO_2 analyte gas molecules, which causes enhancement in sensitivity in the WO_3 nanosheets. The second phenomenon, known as chemical sensitization i.e., the catalytic impact, which happens when the Au nanoparticles size is less than 5 nm. Due to the catalytic process and strong contact seen between NO_2 molecules and hydrocarbons occur from the weakening of Au-Au bonds and the modification of d orbitals as Au nanoparticles size reduces [64]. The oxygen molecules were then encouraged to split apart by the Au doped nanocluster in the WO_3 nanosheets, and the resulting reactive oxygen ions. These oxygen

ions were diffuse into the WO₃ to act as chemical sensitizers. Due to this active site were increased and this process is known as spill-over effect.
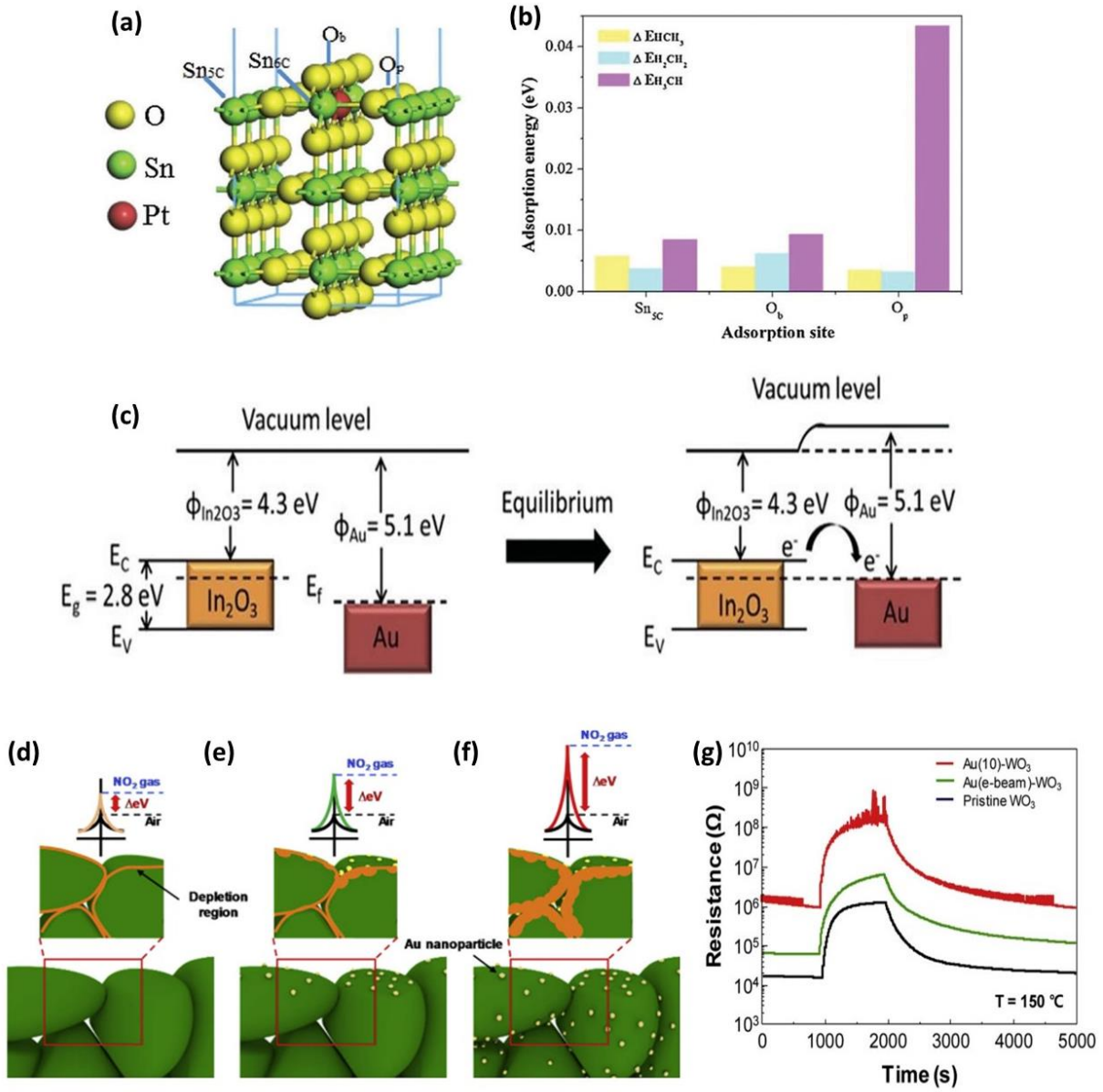

Figure 4. (a) Pt-SnO₂ Computational model, and (b) Different adsorption sites calculated results [3, 49]. (c) Typical band structure of In₂O₃-Au [3, 53]. (d-f) an illustration of the factor contributing to the excellent sensing qualities due to incorporation of Au-doped atoms. (g) The mismatch in the work functions of Au and WO₃, which causes the electrical sensitization, leads to a rise in base resistances [65].

4.2 Doping metals other than noble metals

Another effective way to improve the gas sensitivity is addition of heteroatom doping with another metal. When the metal heteroatom is added to the sensing material then it changes the size, porosity and surface area of the MOS, as a result, gas molecules adsorption sites and diffusion paths are modified [3]. In most of the cases, base atom of the MOS is replaced by the metal heteroatom and causes the reduction in grain size. When the size of the grain is less than twice of the length of the Debye then the entire grain size is occupied by the electron depletion layer. Therefore, the MOS gas sensing property is improved [66-68]. Now, this is not the case that every heteroatom metal doping increased the gas response. As shown in the Figures 5(a) and (b), when atoms of Al, Ga and Zr are added in the In_2O_3 then it improves the response towards formaldehyde [69]. However, when atoms Ti, Mo and W are added in the In_2O_3 then it decreases the material's Fermi level, therefore this has a negative impact on the gas sensing response. Hence for using this specific strategy, it is highly recommended that choose the alternative metal heteroatom for doping into the sensing material very carefully for improving the gas sensing performance [41]. A plausible concept was put out to show how a variation in the Fermi level affects the oxide semiconductor's surface sensitivity and this process was well-known sensing process [64, 70] and explained by theory related to semiconductor physics [71, 72]. This variation in Fermi level is introduced due the absorption of oxygen molecules. Three stages are involved in the sensing process of In_2O_3 nanomaterial to analyze the formaldehyde gas molecules, as depicted in Figures 5(c-e). Firstly, at 150 °C temperature, oxygen molecules present in air get adsorbed on the surface of In_2O_3 nanosheet and consequently withdraw the free electrons from the conduction band, resulting in an upward bending in the energy band diagram. Secondly, under the equilibrium the absorbed oxygen molecule LUMO level and In_2O_3 Fermi level both keep at the same energy level. Lastly, absorbed oxygen combines with formaldehyde gas molecules which causes reduction in energy banding. The energy level mismatch between the semiconductor and adsorbed oxygen molecule combined system in Al-doped In_2O_3 having relatively high Fermi levels (Figures 5 (f-h)) in contrast with undoped In_2O_3, resulting in higher absorption of oxygen molecule on the Al-doped In_2O_3 nanosheet surface in air at equilibrium condition. As a result, Al-doped In_2O_3 responds more strongly towards formaldehyde gas molecules than undoped In_2O_3 because it has more chemisorbed oxygen molecules to respond.
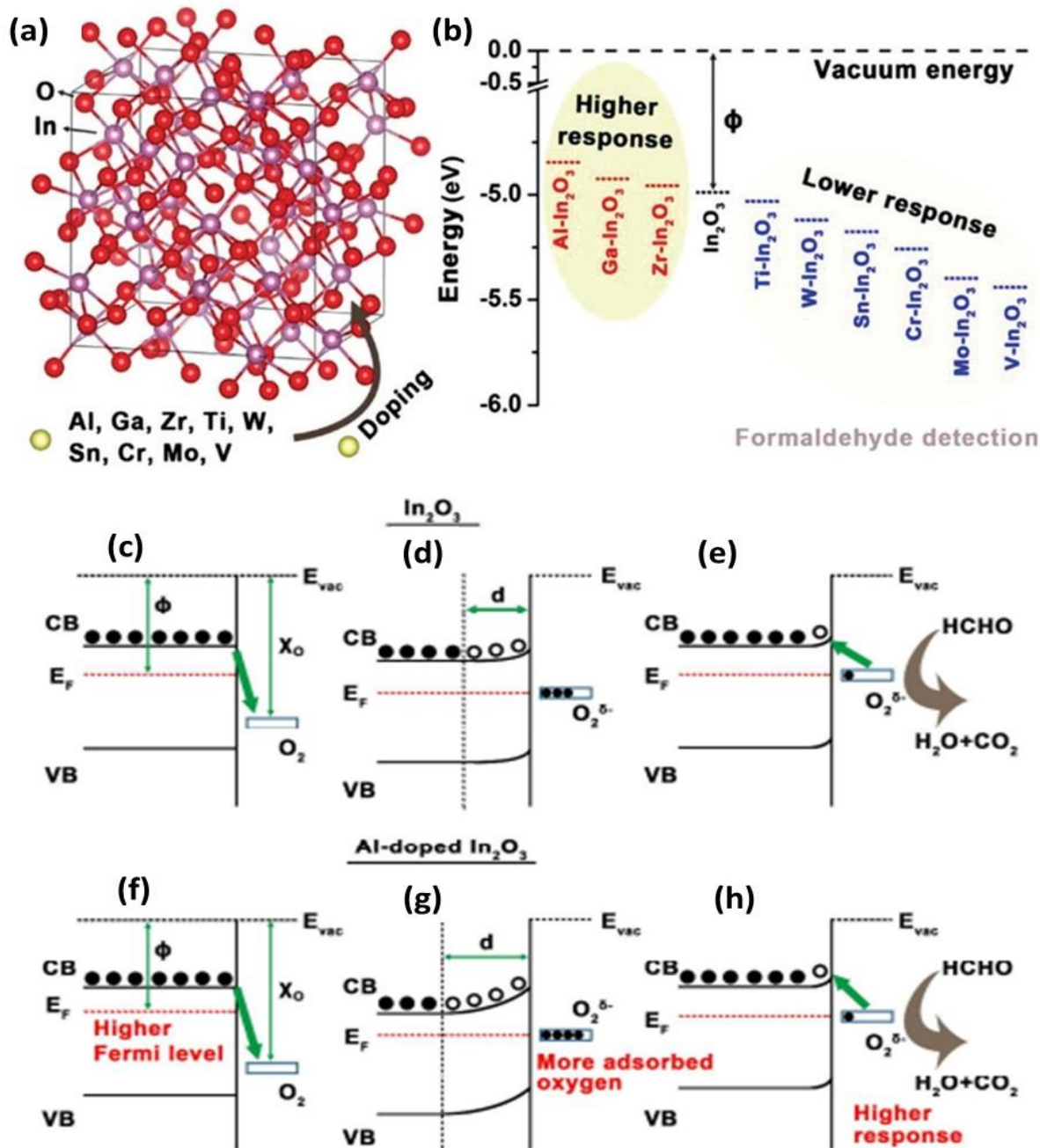
Figure 5. (a) Metal heteroatom-doped In_2O_3 structural model, (b) Fermi levels of ten different kinds of metal heteroatom-doped into the In_2O_3 sensing materials. (c-e) Three stages involved in the sensing process of In_2O_3 nanomaterial to analyze the formaldehyde gas molecules. (f-h) The energy level mismatch between the semiconductor and adsorbed oxygen molecule combined system in Al-doped In_2O_3 having relatively high Fermi levels, in contrast with undoped In_2O_3. [69].

4.3 Developing heterojunctions

Regardless of which sensing material is used, it is nearly impossible to get the maximum of all performance parameters. Therefore, two or more MOS materials are combined to build a heterojunction for overcoming their individual shortcomings. When two distinct materials with different work functions are used for the heterojunction, then the electrons will flow from the lower work function to the higher work function at the interface and this would lead to the electronic depletion and enrichment areas, respectively [73]. The heterojunction gives the appreciative advantage and increase the gas sensing response significantly due to increased catalytic activity and a greater number of available active sites for adsorption of gas molecules. The heterojunctions could be divided into the n-n junctions, p-p junctions, and p-n junctions depending on the type of constituent materials.

The charge carrier dynamics at the heterointerface is explained by Figure 6. When p-n heterojunctions are considered, electrons are transferred from n-type to the p-type MOS and holes are moved in the opposite direction till the nanocomposites Fermi level reaches the equilibrium condition. Therefore, resistance will change at the interface of the heterojunction due to the expansion in electron depletion layer [74]. Now, when material is kept in the reducing gas environment, then target gas and adsorbed O_2 react with each other on the materials surface and electrons returned to the n-type MOS conduction band, as illustrated in Figures 6(a) and (b)[75]. Moreover, some electrons also enter the conduction band of p-type MOS. Consequently, the recombination of electrons and holes will occur, as a result carrier concentration is reduced on either side of the p-n junction [76-78]. Due to the limitation of carrier diffusion, reduction in barrier at the interface is occurred. And apart from that heterojunctions also provides greater adsorption and reaction sites, resulting improved catalytic activity as compared to monomers [79, 80]. Gao et al. have demonstrated the H_2S sensing ability of n-n heterojunction using MoO_3 and SnO_2 MOS [81]. The developed sensor showed high sensitivity and fast response at a lower value of temperature (115 °C) due to larger number of gas adsorption sites at the sensing surface. Upon making physical contact between MoO_3 and SnO_2, electrons started moving from lower work function SnO_2 to higher work function MoO_3. The electrons transfer resulted in bend bending having a barrier height ϕ_{eff}, as shown in Figure 6(c). Upon exposure to H_2S, the trapped electrons

by the oxygen ions and targeted gas molecules, returned to the constituent materials leading to a very high value of sensitivity ascribed to reduction in the potential barrier at the interface.
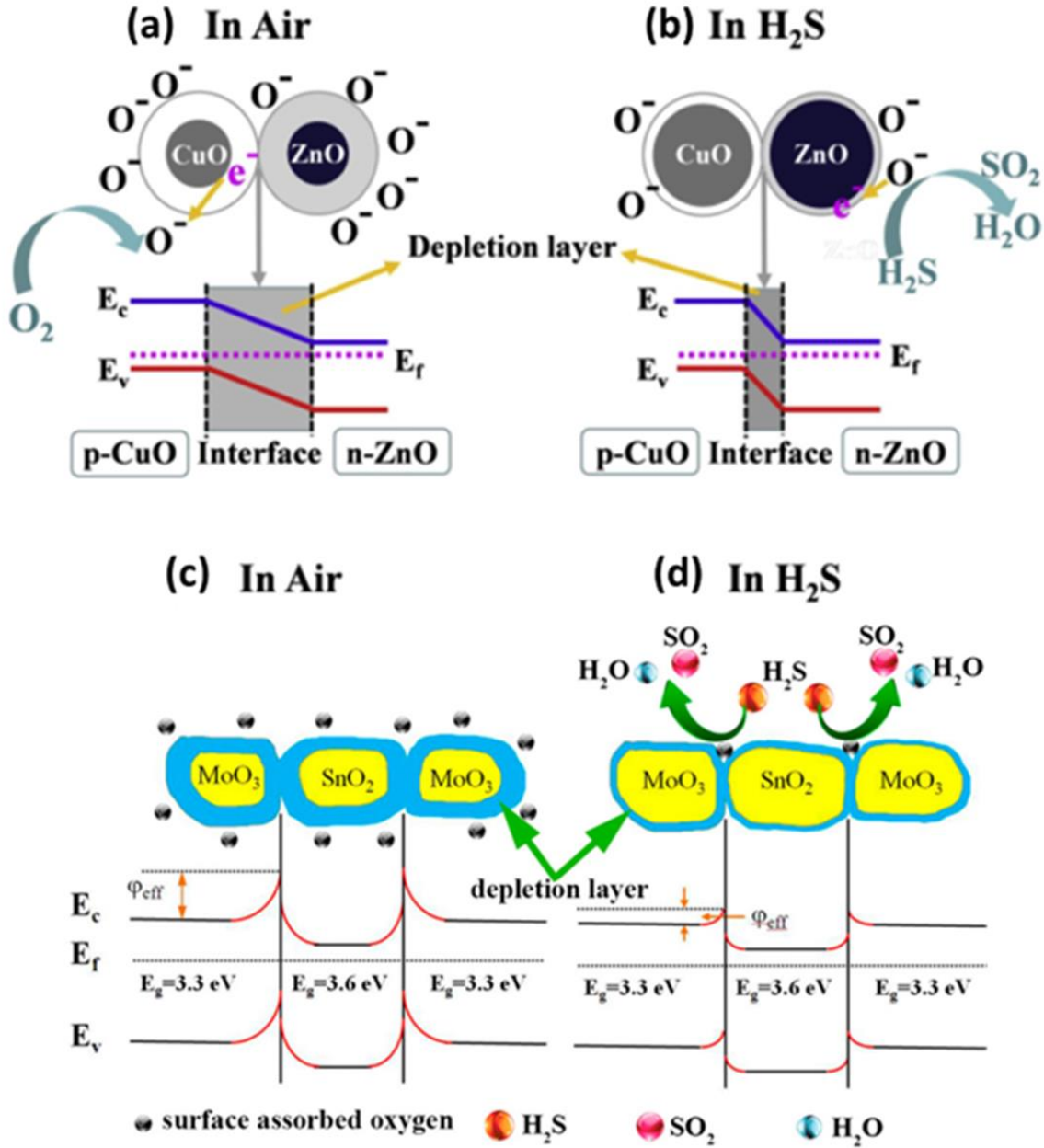

Figure 6. Schematic illustrations of the Energy band diagram at interfaces of (a) p–n, (b) n–nheterojunctions in air and upon exposure of H_2S gas molecules [75, 81].

4.4 MOS modified with the two-dimensional TMDs materials

MX_2 is the general form of transition metal dichalcogenides (TMDs), where M represents the transition metal element (Mo, Ti, etc.) and X refers the chalcogen elements such as S, Se, etc. [82-85]. TMDs is very promising 2D family in the gas sensing applications because of its unique physical and chemical properties. Molybdenum disulphide (MoS_2) and MOS composites are one of the most used composites in the gas sensing applications [47, 86, 87]. Zhang et al. prepared MoS_2 and Co_3O_4 composite sensor with 1 layer, 3 layers, 5 layers and 7 layers on a substrate using layer by layer (LBL) self-assembly method [86]. Upon comparing the sensing performance of all those four different layers composite of MoS_2 and Co_3O_4, it was observed that the five-layer composite gives the best response upon NH_3 exposure at room temperature. They also synthesized MoS_2 and CuO composites by using the LBL technology [87]. By using this sensor they achieved high sensitivity, quick response and excellent stability for H_2S gas molecules [83]. The gas sensing mechanism for this composite is attributed to synergistic effect of energy band structure and creation of p-n heterojunction, as shown in Figures 7(a,b). For better understanding of gas sensing mechanism between H_2S and CuO, X-ray diffraction analysis was performed between MoS_2 and CuO nanocomposites. After exposing to NH_3, some CuS peaks appeared confirming formation of CuS upon CuO and H_2S reaction. Both CuO and MoS_2 have the different work functions and band gaps as depicted in Figures 7(b). Hence, charge transfer will take place until the Fermi level reaches at equilibrium at the heterointerface. The charge distribution forms a depletion layer at the junction and increases the resistance of the composite material. Upon exposure of H_2S, p-type CuO converted into metallic form and the p-n type heterojunction transformed into metal-semiconductor junction as shown in Figure 7(b). This transformation drastically reduces the sensor resistance and hence a very high value of sensitivity was obtained.
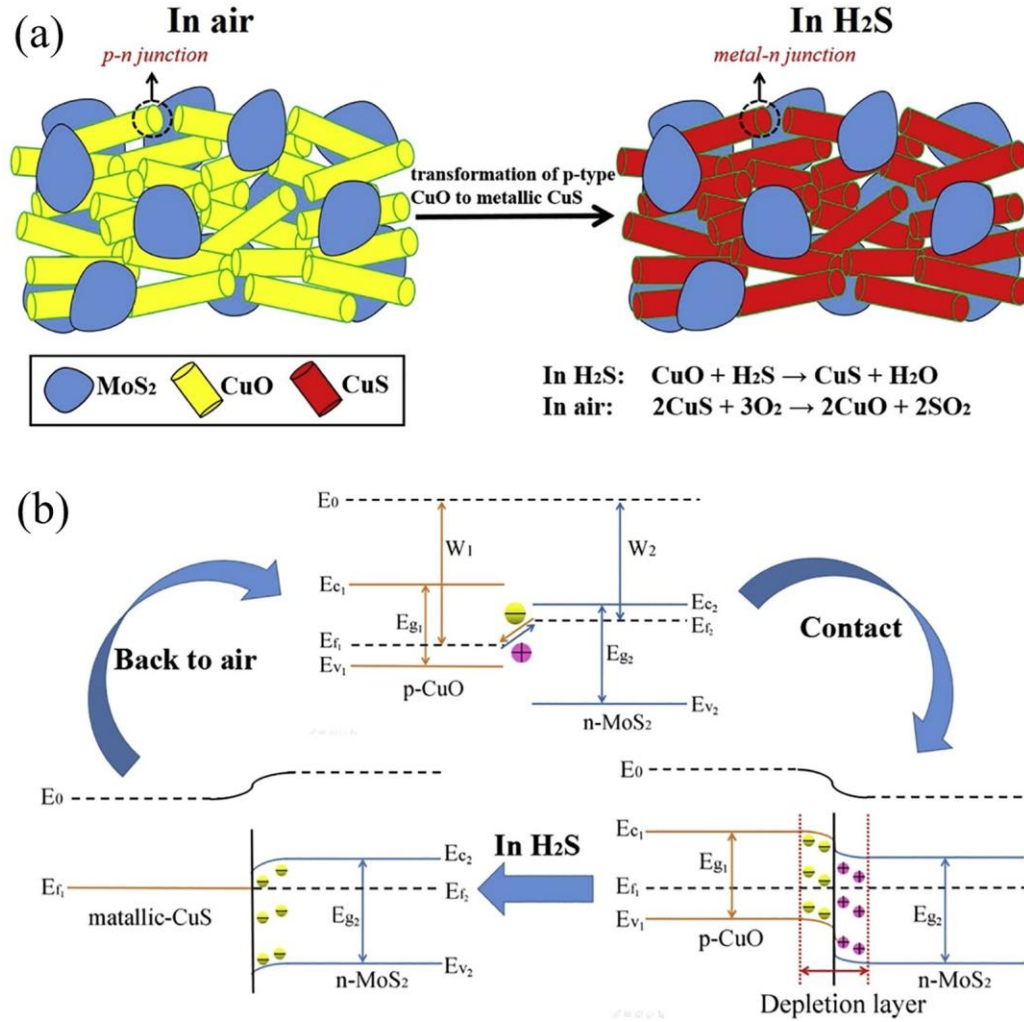
Figure 7. (a) Gas sensing mechanism of H_2S on the composite of CuO and MoS_2. (b) The energy band structure of MoS_2/CuO sensor (here, W_1 and W_2 are the work function, Eg_1 and Eg_2 are the band gap, Ec_1 and Ec_2 are the conduction band bottom, Ev_1 and Ev_2 are the top of valence band and E_f are the Fermi energy level) [87].

4.5 Light induced room temperature gas sensing

Light activation is used as a promising approach in sensing applications for oxide layers such as ZnO, TiO_2, WO_3, etc. [88-90]. In MOS based gas sensing processes, high temperature is required for adsorption and desorption of targeted gas molecules. The energy provided by the external heating element could also be supplied by UV light source resulting in less power consumption and room temperature operation of the developed sensor [91, 92]. In addition, UV light also decrease the measurement time and used for cleaning the gas sensing surface after exposing with

targeted gases [88]. The 1/f noise factor in resistive gas sensors is quite strong and dominates the background noise up to 10 kHz. Figure 8(a) and (b) depicts when potential barriers vary between the grain's boundaries, it leads to the generation of low-frequency noise. The gas sensor's temperature and surrounding atmosphere can be specifically affected by the barrier's variations because it relies on the adsorption and desorption mechanisms. The 1/f noise is shown to rise with decreasing grain size in experimental data. Furthermore, when gas-sensor nanomaterial grain size reduces, the sensitivity of sensor get enhanced and noise fluctuations becomes even more sensitive than that of variations in DC resistance [93].

Smulko et al. have discussed the application of photo activation for improving the gas sensing ability of the sensors at lower value of operating temperature[94]. The recorded data are shown in the Figures 8(c) and (d) when Au is decorated on the WO_3 sensing layer. The change in DC resistance (Rs) of sensor is compared after the increment in heating voltage upon UV irradiation (365 nm) by the help of T5F UV diode [95]. This diode was placed approximately 5 mm away from the sensing layer and its DC current (Id) was controllable up to a maximum of 20 mA. This recorded curve shape depends on the surrounding atmosphere as this was examined for synthetic air (Figure 8(c)) and ethanol (Figure 8(d)). It was observed that the recorded data is quite similar for both the cases whether it was UV light or temperature modulation [94]. But one thing is very noticeable that power consumption is lesser in UV light than the power required for temperature modulation (even at lower value of Id, change in DC resistance of sensor may be seen in Figure 8(d)). Hence, by using the UV light, sensor can work at lower temperature, which is very appealing characteristic [94].
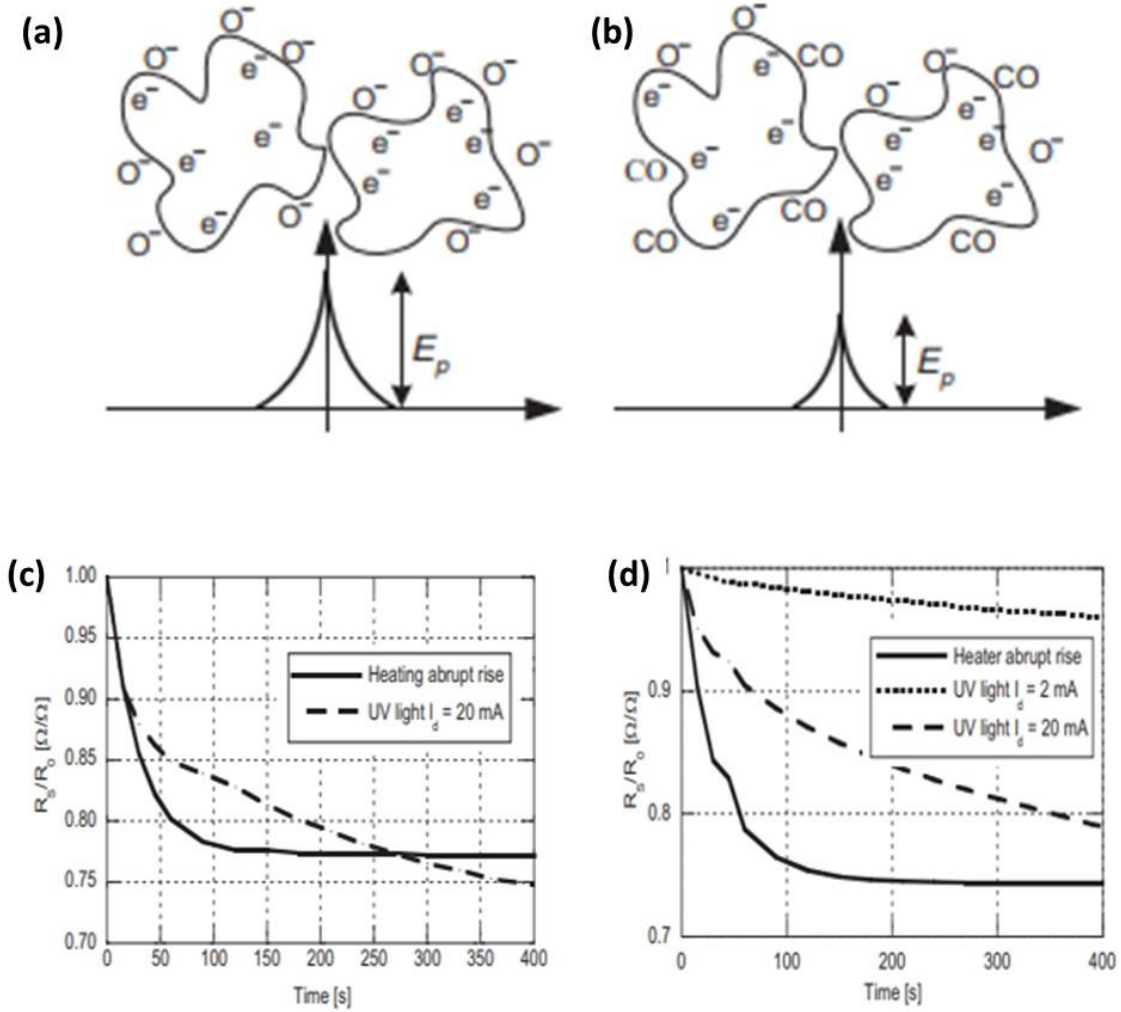
Figure 8. (a) and (b) depicts when potential barriers vary in between the grain's boundaries, it leads in the generation of low-frequency noise. Relative change in Rs for gas sensing layer WO_3 when heating voltage change from 1.5 V to 1.8 V, corresponding to the change in temperature between 100°C and 120°C: (c) Ro denotes the resistance in the synthetic air at the 1.5 V heating voltage, (d) data were taken in ethanol (200 ppm) and Ro denotes the resistance in the 200 ppm of ethanol at 1.5 V heating voltage [94].

4.6 Nanostructures with exposed facets

Nanostructured exposed crystal facets exhibit large difference in their gas sensing abilities because of their distinct surface properties. The crystal facets with more defect sites possess a higher value of surface energy, therefore they have more active physicochemical features [96-98]. Exposed crystal facets of MOS materials have been used very often in the photocatalysis and

recently MOS materials have also showed enormous potential in the realm of gas sensing [99, 100]. Overall, the improvement in gas adsorption ascribed to greater density value of dangling bonds and coordination of unsaturated oxygen. For example, upon observing every crystal planes atomic structure diagram of ZnO and calculating the densities of dangling bond of every plane, it revealed that the crystal plane (0001) has higher density [17]. Dangling bonds due to the Zn^{2+} have unsaturated O_2 coordination on the surface and when the gas sensing reaction starts then target gases and O_2 anions are adsorbed at these locations. Kaneti et al. [101] used density function theory to examine the ZnO sensing response upon exposure to ethanol. They observed that the exposed crystal plane (0001) interacted with the surface oxygen, the H-O bonds are then shortened and recuces the adsorption energy. Hence, in the case of (0001) crystal plane, an excellent gas sensitivity could be obtained [17].

When target gas and sensing materials surface comes in contact, then there is a higher charge transfer and stronger electron interaction between the target gas and the high energy crystal facet resulting in quicker and greater gas response, as shown in Figures 9(a) and (b)[102]. To investigate the selectivity of particular gases (such as acetone, ethanol, H_2, H_2S, NH_3, NO_2), the responses of several nanocrystals to distinct gases each having concentration level of 100 ppm at 320 °C were examined as shown in Figure 9(c). It was discovered that NS-010 displays a noticeably stronger acetone response when contrasted to other gases, demonstrating superior acetone sensing selectivity, whereas NS-101 (NS denoted TiO_2 nanocrystals with anatase have been fabricated with different facets) displays a substantially lower acetone selectivity. The outcomes showed that the crystal facet tuning can be used to achieve selective recognition for the acetone. At concentration level of 100 ppm acetone response was measured on the TiO_2 nanosheet as sensing materials, and this experiment were conducted continuously for 15 days in order to examine stability as shown in Figure 9(d). the obtained results showed a great consistency of the TiO_2 nanostructures, as evident from the fact that both NS-010 and NS-101 sustain about 95% of the initial reaction even afterwards being tested for 15 days.
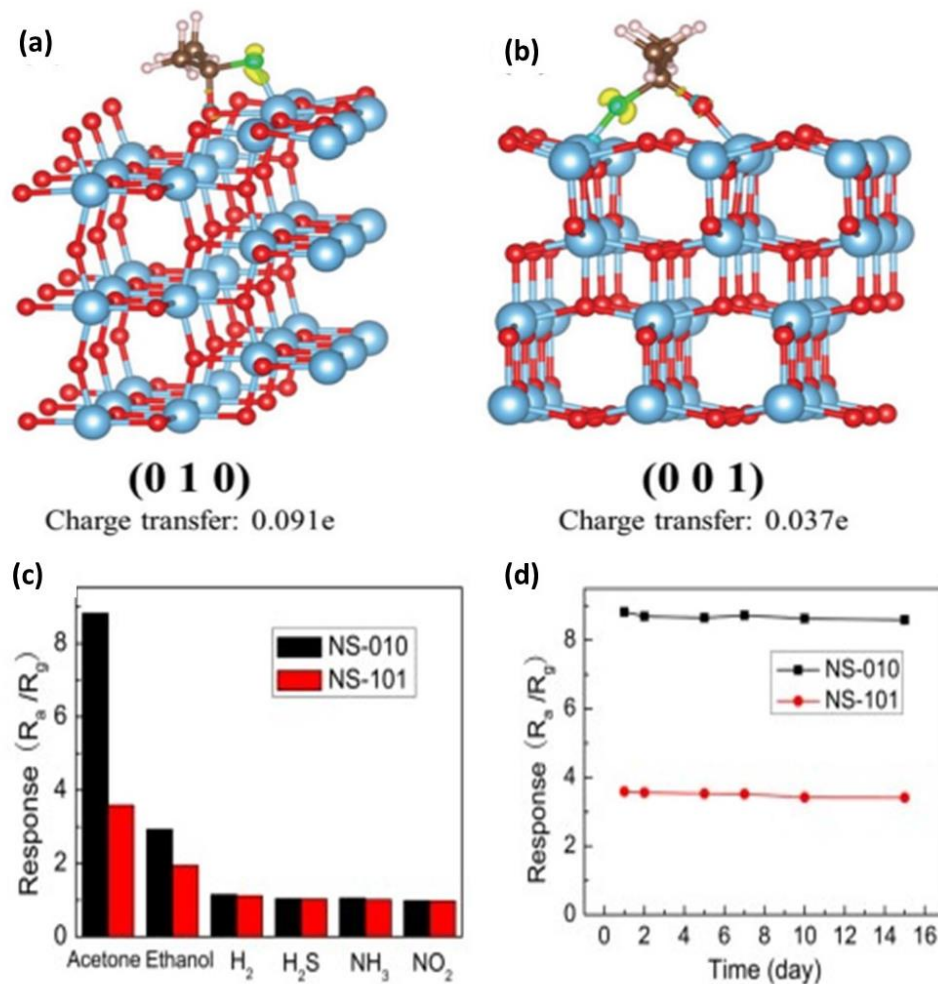
Figure 9. Schematic diagram of charge transfer between a target gas molecule and facets (a) TiO$_2$ (010) and (b) TiO$_2$ (001). (c). the responses of several nanocrystals to distinct gases each having concentration level of 100 ppm at 320 °C were examined. (d). At concentration level of 100 ppm acetone response was measured on the TiO$_2$ nanosheet as sensing materials, and this experiment were conducted continuously for 15 days in order to examine stability [102].

5. Conclusion and perspectives

The MOS has been the focal point for developing efficient gas sensors due to their inherent characteristics. This review paper provides the in-depth knowledge of different type of gas sensing mechanism and different type of methods responsible for improvement of gas sensing. We have also discussed about different kinds of MOS nanostructures such as nanorods, nanobelts, nanofibers, nanosheets, and their composites. The recent progress in sensing

mechanism for detecting different kinds of hazardous and flammable gases including NO_2, NH_3, H_2S, H_2, and volatile organic compounds have also been summarized.

The study of MOS based gas sensor still faces many opportunities and challenges. There are still some questions which can't be explained by using the existing gas sensing mechanism. Therefore, it is necessary to do more research in this topic for the better understanding of the topic. In this area more experiments are required using the modern technique such as situ analysis to know about the effect of different type of gas sensing mechanism on the performance of gas sensors. By studying the unexplored physics, we can select the appropriate and accurate gas sensing mechanism in future.

The chemisorbed oxygen species on the MOS surface slow down the desorption process and requires some external energy to improve the speed of the sensor. Thermal and photo energy appears to be the most widely used external sources to expedite the desorption mechanism. However, these techniques increase the power consumption and restrict the portability of the sensor. Research on the topic of MOS based gas sensor is increasing day by day, but attention paid to this topic is still not sufficient, therefore most paper have failed to give accurate information regarding the role of heterojunction in the gas sensing, gas sensing mechanism and the best material for sensing particular gases.

Conflicts of interest

There are no conflicts to declare.

References

[1]   V. Blazy, A. de Guardia, J. C. Benoist, M. Daumoin, F. Guiziou, M. Lemasle, D. Wolbert, S. Barrington, *Chemical Engineering Journal* **2015**, 276, 398.

[2]   A. Tricoli, M. Righettoni, A. Teleki, *Angewandte Chemie International Edition* **2010**, 49, 7632.

[3]   H. Ji, W. Zeng, Y. Li, *Nanoscale* **2019**, 11, 22664.

[4]   T. Anukunprasert, C. Saiwan, E. Traversa, *Science and Technology of Advanced Materials* **2005**, 6, 359.

[5]   A. Dey, *Materials Science and Engineering: B* **2018**, 229, 206.

[6]   G. Eranna, B. Joshi, D. Runthala, R. Gupta, *Critical Reviews in Solid State and Materials Sciences* **2004**, 29, 111.

[7]   H. Ji, W. Zeng, Y. Li, *Physica E: Low-dimensional Systems and Nanostructures* **2019**, 114, 113646.

[8]   W. Tang, H. Liu, C. Li, Y. Zhang, H. Sun, T. Peng, J. Huo, *Journal of Physics and Chemistry of Solids* **2019**, 134, 5.

[9]   X. Chen, S. S. Mao, *Chemical reviews* **2007**, 107, 2891.

[10]   L. Zhu, W. Zeng, *Sensors and Actuators A: Physical* **2017**, 267, 242.

[11]   Y. Zhang, D. Li, L. Qin, P. Zhao, F. Liu, X. Chuai, P. Sun, X. Liang, Y. Gao, Y. Sun, *Sensors and Actuators B: Chemical* **2018**, 255, 2944.

[12]   J. Shen, S. Guo, C. Chen, L. Sun, S. Wen, Y. Chen, S. Ruan, *Sensors and Actuators B: Chemical* **2017**, 252, 757.

[13]   R. Lü, W. Zhou, K. Shi, Y. Yang, L. Wang, K. Pan, C. Tian, Z. Ren, H. Fu, *Nanoscale* **2013**, 5, 8569.

[14]   H. Long, W. Zeng, H. Zhang, *Journal of Materials Science: Materials in Electronics* **2015**, 26, 4698.

[15]   B. Liu, L. Wang, Y. Ma, Y. Yuan, J. Yang, M. Wang, J. Liu, X. Zhang, Y. Ren, Q. Du, *Applied Surface Science* **2019**, 470, 596.

[16]   Q. Guo, Y. Li, W. Zeng, *Physica E: Low-dimensional Systems and Nanostructures* **2019**, 114, 113564.

[17]   X. Gao, T. Zhang, *Sensors and Actuators B: Chemical* **2018**, 277, 604.

[18]   D. Kwak, Y. Lei, R. Maric, *Talanta* **2019**, 204, 713.

[19]   G. Neri, N. Donato, *Wiley encyclopedia of electrical and electronics engineering* **1999**, 1.

[20]   P. Gründler, *Chemical sensors: an introduction for scientists and engineers*, Springer Science & Business Media, **2007**.

[21]   J. Huang, Q. Wan, *Sensors* **2009**, 9, 9903.

[22]   X. Liu, S. Cheng, H. Liu, S. Hu, D. Zhang, H. Ning, *Sensors* **2012**, 12, 9635.

[23]   G. Korotcenkov, *Materials Science and Engineering: B* **2007**, 139, 1.

[24]   J. R. DeBoer, Georgia Institute of Technology, 2004.

[25]   S. Wendt, R. Schaub, J. Matthiesen, E. K. Vestergaard, E. Wahlström, M. D. Rasmussen, P. Thostrup, L. Molina, E. Lægsgaard, I. Stensgaard, *Surface Science* **2005**, 598, 226.

[26]   P. Moseley, *Sensors and Actuators B: Chemical* **1992**, 6, 149.

[27]   R. S. Andre, J. C. Pereira, L. A. Mercante, D. Locilento, L. H. Mattoso, D. S. Correa, *Journal of Alloys and Compounds* **2018**, 767, 1022.

[28]   S. Singh, G. Gupta, S. Yadav, P. Dubey, V. Ojha, A. Kumar, *Sensors and Actuators A: Physical* **2019**, 295, 133.

[29]   L. Wang, F. Zhao, Q. Han, C. Hu, L. Lv, N. Chen, L. Qu, *Nanoscale* **2015**, 7, 9694.

[30]   H. Yu, S. Gao, X. Cheng, P. Wang, X. Zhang, Y. Xu, H. Zhao, L. Huo, *Sensors and Actuators B: Chemical* **2019**, 297, 126744.

[31]   Y. Deng, in *Semiconducting Metal Oxides for Gas Sensing*, Springer, 2019.

[32]   M. Wang, T. Hou, Z. Shen, X. Zhao, H. Ji, *Sensors and Actuators B: Chemical* **2019**, 292, 171.

[33]   M. Yang, X. Liu, X. Zhao, B. Li, X. Wang, *Chem. Res. Chin. Univ* **2014**, 35, 1615.

[34]   G. Gao, J. Wu, G. Wu, Z. Zhang, W. Feng, J. Shen, B. Zhou, *Sensors and Actuators B: Chemical* **2012**, 171, 1288.

[35]   D. Williams, G. Henshaw, K. Pratt, R. Peat, *Journal of the Chemical Society, Faraday Transactions* **1995**, 91, 4299.

[36]   H. Lu, W. Ma, J. Gao, J. Li, *Sensors and Actuators B: Chemical* **2000**, 66, 228.

[37]   G. Sakai, N. Matsunaga, K. Shimanoe, N. Yamazoe, *Sensors and Actuators B: Chemical* **2001**, 80, 125.

[38]   X. Wang, Y. Wang, F. Tian, H. Liang, K. Wang, X. Zhao, Z. Lu, K. Jiang, L. Yang, X. Lou, *The Journal of Physical Chemistry C* **2015**, 119, 15963.

[39]   S. Mohammad-Yousefi, S. Rahbarpour, H. Ghafoorifard, *Materials Chemistry and Physics* **2019**, 227, 148.

[40]   K. Selvaraj, S. Kumar, R. Lakshmanan, *Ain Shams Engineering Journal* **2014**, 5, 885.

[41]   S. Yang, Z. Wang, Y. Zou, X. Luo, X. Pan, X. Zhang, Y. Hu, K. Chen, Z. Huang, S. Wang, *Sensors and Actuators B: Chemical* **2017**, 248, 160.

[42]   S. M. Majhi, H.-J. Lee, H.-N. Choi, H.-Y. Cho, J.-S. Kim, C.-R. Lee, Y.-T. Yu, *CrystEngComm* **2019**, 21, 5084.

[43]   Q. Sun, J. Wang, J. Hao, S. Zheng, P. Wan, T. Wang, H. Fang, Y. Wang, *Nanoscale* **2019**, 11, 13741.

[44]   Y. Guo, X. Tian, X. Wang, J. Sun, *Sensors and Actuators B: Chemical* **2019**, 293, 136.

[45]   L. A. Mercante, R. S. Andre, L. H. Mattoso, D. S. Correa, *ACS Applied Nano Materials* **2019**, 2, 4026.

[46]   H. Ji, W. Zeng, Y. Li, *Materials Research Bulletin* **2019**, 118, 110476.

[47]   E. Lee, Y. S. Yoon, D.-J. Kim, *ACS sensors* **2018**, 3, 2045.

[48]   R. Zhou, X. Lin, D. Xue, F. Zong, J. Zhang, X. Duan, Q. Li, T. Wang, *Sensors and Actuators B: Chemical* **2018**, 260, 900.

[49]   D. Xue, P. Wang, Z. Zhang, Y. Wang, *Sensors and Actuators B: Chemical* **2019**, 296, 126710.

[50]   L. Mädler, A. Roessler, S. E. Pratsinis, T. Sahm, A. Gurlo, N. Barsan, U. Weimar, *Sensors and Actuators B: Chemical* **2006**, 114, 283.

[51]   M. Zhang, Z. Yuan, J. Song, C. Zheng, *Sensors and Actuators B: Chemical* **2010**, 148, 87.

[52]   M. Yuasa, T. Masaki, T. Kida, K. Shimanoe, N. Yamazoe, *Sensors and Actuators B: Chemical* **2009**, 136, 99.

[53]   X. Yang, H. Fu, Y. Tian, Q. Xie, S. Xiong, D. Han, H. Zhang, X. An, *Sensors and Actuators B: Chemical* **2019**, 296, 126696.

[54]   T. H. Kim, W. Sohn, J. M. Suh, Y.-S. Shim, K. C. Kwon, K. Hong, S. Choi, H.-G. Byun, J.-H. Lee, H. W. Jang, *Sensors and Actuators B: Chemical* **2018**, 274, 587.

[55]   Y.-S. Shim, H. Y. Jeong, Y. H. Kim, S. H. Nahm, C.-Y. Kang, J.-S. Kim, W. Lee, H. W. Jang, *Sensors and Actuators B: Chemical* **2015**, 213, 314.

[56]   R.-J. Ma, X. Zhao, X. Zou, G.-D. Li, *Journal of Alloys and Compounds* **2018**, 732, 863.

[57]   S. J. Ippolito, S. Kandasamy, K. Kalantar-Zadeh, W. Wlodarski, *Sensors and Actuators B: Chemical* **2005**, 108, 154.

[58]   T. Maosong, D. Guorui, G. Dingsan, *Applied surface science* **2001**, 171, 226.

[59]   P. Dwivedi, N. Chauhan, P. Vivekanandan, S. Das, D. S. Kumar, S. Dhanekar, *Sensors and Actuators B: Chemical* **2017**, 249, 602.

[60]   P. Dwivedi, S. Dhanekar, S. Das, *Nanotechnology* **2018**, 29, 275503.

[61]   E. Comini, G. Faglia, G. Sberveglieri, Z. Pan, Z. L. Wang, *Applied physics letters* **2002**, 81, 1869.

[62]   M. Penza, C. Martucci, G. Cassano, *Sensors and Actuators B: Chemical* **1998**, 50, 52.

[63]   Y. Shen, H. Bi, T. Li, X. Zhong, X. Chen, A. Fan, D. Wei, *Applied surface science* **2018**, 434, 922.

[64]   C. Wang, L. Yin, L. Zhang, D. Xiang, R. Gao, *sensors* **2010**, 10, 2088.

[65]   T. H. Kim, A. Hasani, Y. Kim, S. Y. Park, M. G. Lee, W. Sohn, T. P. Nguyen, K. S. Choi, S. Y. Kim, H. W. Jang, *Sensors and Actuators B: Chemical* **2019**, 286, 512.

[66]   H. Chen, J. Hu, G.-D. Li, Q. Gao, C. Wei, X. Zou, *ACS applied materials & interfaces* **2017**, 9, 4692.

[67]   G. K. Mani, J. B. B. Rayappan, *Journal of alloys and compounds* **2014**, 582, 414.

[68]   G. K. Mani, J. B. B. Rayappan, *Sensors and Actuators B: Chemical* **2016**, 223, 343.

[69]   H. Chen, Y. Zhao, L. Shi, G.-D. Li, L. Sun, X. Zou, *ACS applied materials & interfaces* **2018**, 10, 29795.

[70]   M. E. Franke, T. J. Koplin, U. Simon, *small* **2006**, 2, 36.

[71]   Z. Zhang, J. T. Yates Jr, *Chemical reviews* **2012**, 112, 5520.

[72]   A. Akbashev, L. Zhang, J. Mefford, J. Park, B. Butz, H. Luftman, W. Chueh, A. Vojvodic, *Energy & Environmental Science* **2018**, 11, 1762.

[73]   J. M. Walker, S. A. Akbar, P. A. Morris, *Sensors and Actuators B: Chemical* **2019**, 286, 624.

[74]   A. Bag, N.-E. Lee, *Journal of Materials Chemistry C* **2019**, 7, 13367.

[75]   C. Han, X. Li, C. Shao, X. Li, J. Ma, X. Zhang, Y. Liu, *Sensors and Actuators B: Chemical* **2019**, 285, 495.

[76]   Z. Li, H. Li, Z. Wu, M. Wang, J. Luo, H. Torun, P. Hu, C. Yang, M. Grundmann, X. Liu, *Materials Horizons* **2019**, 6, 470.

[77]   X. Zhou, X. Cheng, Y. Zhu, A. A. Elzatahry, A. Alghamdi, Y. Deng, D. Zhao, *Chinese Chemical Letters* **2018**, 29, 405.

[78]   J. Liu, M. Dai, T. Wang, P. Sun, X. Liang, G. Lu, K. Shimanoe, N. Yamazoe, *ACS applied materials & interfaces* **2016**, 8, 6669.

[79]   Y. Wang, Y. Zhou, C. Meng, Z. Gao, X. Cao, X. Li, L. Xu, W. Zhu, X. Peng, B. Zhang, *Nanotechnology* **2016**, 27, 425503.

[80]   Y. Cao, Y. He, X. Zou, G.-D. Li, *Sensors and Actuators B: Chemical* **2017**, 252, 232.

[81]   X. Gao, Q. Ouyang, C. Zhu, X. Zhang, Y. Chen, *ACS Applied Nano Materials* **2019**, 2, 2418.

[82]   N. Chaudhary, M. Khanuja, *Journal of The Electrochemical Society* **2019**, 166, B1276.

[83]   D. Zhang, Z. Yang, S. Yu, Q. Mi, Q. Pan, *Coordination Chemistry Reviews* **2020**, 413, 213272.

[84]   L. Zhang, K. Khan, J. Zou, H. Zhang, Y. Li, *Advanced Materials Interfaces* **2019**, 6, 1901329.

[85]   C. Tan, X. Cao, X.-J. Wu, Q. He, J. Yang, X. Zhang, J. Chen, W. Zhao, S. Han, G.-H. Nam, *Chemical reviews* **2017**, 117, 6225.

[86]   D. Zhang, C. Jiang, P. Li, Y. e. Sun, *ACS applied materials & interfaces* **2017**, 9, 6462.

[87]   D. Zhang, J. Wu, Y. Cao, *Sensors and Actuators B: Chemical* **2019**, 287, 346.

[88]   E. Comini, A. Cristalli, G. Faglia, G. Sberveglieri, *Sensors and Actuators B: Chemical* **2000**, 65, 260.

[89]   Z. Topalian, J. Smulko, G. A. Niklasson, C. G. Granqvist, presented at *Journal of physics: Conference series*, **2007**.

[90]   X. Dong, Y. Ma, G. Zhu, Y. Huang, J. Wang, M. B. Chan-Park, L. Wang, W. Huang, P. Chen, *Journal of Materials Chemistry* **2012**, 22, 17044.

[91]   N. D. Chinh, N. D. Quang, H. Lee, T. Thi Hien, N. M. Hieu, D. Kim, C. Kim, D. Kim, *Scientific reports* **2016**, 6, 1.

[92]   G. Chen, T. M. Paronyan, E. M. Pigos, A. R. Harutyunyan, *Scientific reports* **2012**, 2, 1.

[93]   J. Ederth, J. Smulko, L. B. Kish, P. Heszler, C. G. Granqvist, *Sensors and Actuators B: Chemical* **2006**, 113, 310.

[94]   J. M. Smulko, M. Trawka, C. G. Granqvist, R. Ionescu, F. Annanouch, E. Llobet, L. B. Kish, *Sensor Review* **2015**.

[95]   S. Vallejos, P. Umek, T. Stoycheva, F. Annanouch, E. Llobet, X. Correig, P. De Marco, C. Bittencourt, C. Blackman, *Advanced Functional Materials* **2013**, 23, 1313.

[96]   Z. Wang, J. Xue, D. Han, F. Gu, *ACS Applied Materials & Interfaces* **2015**, 7, 308.

[97]   J. Liu, G. Chen, Y. Yu, Y. Wu, M. Zhou, H. Zhang, C. Lv, Y. Zheng, F. He, *RSC Advances* **2015**, 5, 44306.

[98]   Z. Xie, N. Han, W. Li, Y. Deng, S. Gong, Y. Wang, X. Wu, Y. Li, Y. Chen, *physica status solidi (a)* **2017**, 214, 1600904.

[99]   G. Zhu, X. Yu, F. Xie, W. Feng, *Applied Surface Science* **2019**, 485, 496.

[100]   W. Chen, Q. Liu, S. Tian, X. Zhao, *Applied Surface Science* **2019**, 470, 807.

[101]   Y. V. Kaneti, Z. Zhang, J. Yue, Q. M. Zakaria, C. Chen, X. Jiang, A. Yu, *Physical Chemistry Chemical Physics* **2014**, 16, 11471.

[102]   Y. Liang, Y. Yang, H. Zhou, C. Zou, K. Xu, X. Luo, T. Yu, W. Zhang, Y. Liu, C. Yuan, *Ceramics International* **2019**, 45, 6282.